



Two reductases complete steroidal glycoalkaloids biosynthesis in potato

Akiyama, Ryota ; Terami, Daiki ; Noda, Aozora ; Watanabe, Bunta ;
Umemoto, Naoyuki ; Muranaka, Toshiya ; Saito, Kazuki ; Sugimoto, ...

(Citation)

New Phytologist, 245(6):2632-2644

(Issue Date)

2025-03

(Resource Type)

journal article

(Version)

Version of Record

(Rights)

© 2025 The Author(s). New Phytologist

© 2025 New Phytologist Foundation








This is an open access article under the terms of the Creative Commons Attribution-NonCommercial-NoDerivs License, which permits use and distribution in any medium, ...

(URL)

<https://hdl.handle.net/20.500.14094/0100492919>



Two reductases complete steroidal glycoalkaloids biosynthesis in potato

Ryota Akiyama¹ , Daiki Terami¹, Aozora Noda¹, Bunta Watanabe² , Naoyuki Umemoto³ ,
Toshiya Muranaka⁴ , Kazuki Saito³ , Yukihiro Sugimoto¹  and Masaharu Mizutani¹ 

¹Graduate School of Agricultural Science, Kobe University, Rokkoudai 1-1, Nada, Kobe, Hyogo, 657-8501, Japan; ²The Jikei University School of Medicine, 8-3-1 Kokuryo, Chohu, Tokyo, 182-8570, Japan; ³RIKEN Center for Sustainable Resource Science, Suchoi-cho 1-7-22, Tsurumi-ku, Yokohama, Kanagawa, 230-0045, Japan; ⁴Department of Biotechnology, Graduate School of Engineering, Osaka University, Yamadaoka 2-1, Suita, Osaka, 565-0871, Japan

Authors for correspondence:

Ryota Akiyama

Email: ryota.akiyama@riken.jp

Masaharu Mizutani

Email: mizutani@gold.kobe-u.ac.jp

Received: 16 September 2024

Accepted: 6 January 2025

New Phytologist (2025)

doi: 10.1111/nph.20411

Key words: RPG1, RPG2, Solanaceae, steroidal glycoalkaloids (SGAs), α -solanine.

Summary

- Steroidal glycoalkaloids (SGAs) are specialized metabolites primarily produced by Solanaceae plants such as potatoes and tomatoes. Notably, α -solanine and α -chaconine are recognized as toxic substances in potatoes. While the biosynthetic pathways of SGAs are largely understood, the final steps of α -solanine and α -chaconine biosynthesis remained elusive.
- In this study, we discovered that two reductase-encoding genes, reductase for potato glycoalkaloid biosynthesis 1 (RPG1) and RPG2, complete SGA biosynthesis in potato. Knockout of both RPG1 and RPG2 in potato hairy roots halted α -solanine production, leading to the accumulation of zwitter-solanine.
- We analyzed the catalytic function of recombinant enzymes and conducted structural determination of the reaction products by nuclear magnetic resonance. As a result, RPG1 converted zwitter-solanine to 16-iminiumsolanine, and RPG2 further converted it to α -solanine. RPG2 also transformed zwitter-solanine to 22-iminiumsolanine, which RPG1 then converted to α -solanine. Similar processes were observed for α -chaconine synthesis from zwitter-chaconine. Due to differences in enzymatic reaction efficiency, the biosynthetic pathway via 16-iminiumsolanine/16-iminiumchaconine was suggested to be predominant in potato.
- Our results could pave the way for tailoring SGA structures within Solanum plants, enabling the development of Solanum crop varieties with reduced toxicity or enhanced resistance to diseases and pests.

Introduction

Steroidal glycoalkaloids (SGAs), a class of specialized metabolites derived from cholesterol and containing nitrogen, are typically found in the Solanaceae plant family. This includes staple food crops such as potato (*Solanum tuberosum*), tomato (*Solanum lycopersicum*), and eggplant (*Solanum melongena*) (Friedman, 2002, 2006, 2015). SGAs serve as a chemical protectant against a wide range of plant pathogens and herbivores (Milner *et al.*, 2011). Some SGAs are considered antinutritional factors in foods, causing gastrointestinal and neurological disorders in humans, in addition to exhibiting unpleasant tastes described as bitter, burning, scratchy, or acrid.

SGAs are composed of two structural elements: the aglycone unit, an anitrogen-containing steroid derived from cholesterol, and a glycoside residue attached to the hydroxy group at C-3 (Milner *et al.*, 2011; Sawai *et al.*, 2014). The skeletal structure of the aglycone allows SGAs to be classified into two general classes: spiro-solane and solanidane (Friedman *et al.*, 1997; Milner *et al.*, 2011). Tomatoes exclusively contain spiro-solane-type

SGAs, with α -tomatine and dehydrotomatine being the most abundant in green tissues (Friedman, 2002). Conversely, potatoes produce solanidane-type SGAs, specifically α -solanine and α -chaconine, which constitute over 90% of the total SGAs in cultivated potatoes (Shakya & Navarre, 2008).

Recent research on tomato and potato plants has uncovered numerous biosynthetic genes involved in SGA biosynthesis (Fig. 1). Three cytochrome P450 monooxygenases (PGA2/GAME6, PGA1/GAME8, and PGA3/GAME4), a 2-oxoglutarate-dependent dioxygenase (16DOX/GAME11), and an aminotransferase (PGA4/GAME12) have been identified as key players in the early stages of SGA biosynthesis from cholesterol (Itkin *et al.*, 2013; Umemoto *et al.*, 2016; Nakayasu *et al.*, 2017, 2021). Additionally, GAME15, a member of the cellulose synthase-like family, has been identified as an SGA biosynthetic gene (Jozwiak *et al.*, 2024). GAME15 catalyzes the transglucuronidation of the C3-hydroxy group of cholesterol, which represents the first step in the SGA biosynthetic pathway from cholesterol (Jozwiak *et al.*, 2024). Furthermore, GAME15 functions as a scaffold protein, facilitating physical interactions among the SGA biosynthetic

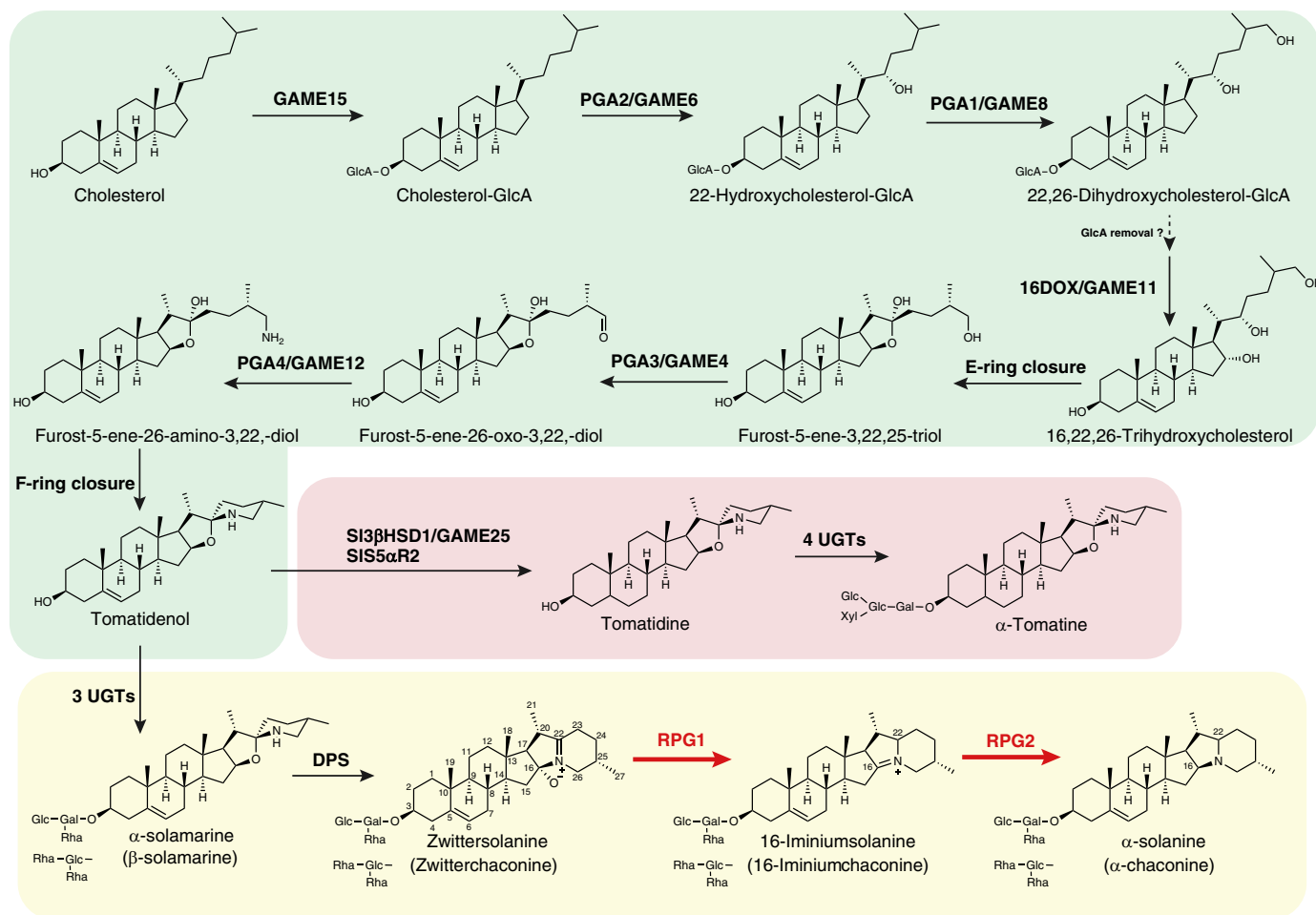


Fig. 1 Steroidal glycoalkaloids biosynthetic pathway in potato (*Solanum tuberosum*) and tomato (*Solanum lycopersicum*). Common steps between potato and tomato are highlighted in green. Steps unique to tomato or potato are indicated by red or yellow shading, respectively. The reaction step characterized in this work by reductase for potato glycoalkaloids biosynthesis enzymes, is shown with a red arrow. 16DOX, 22,26-hydroxycholesterol 16 α -hydroxylase; 3 β HSD1, 3 β -hydroxysteroid dehydrogenases 1; UGT, uridine diphosphate-dependent glycosyltransferases; Xyl, xylose; Gal, galactose; GAME, glycoalkaloids metabolism; Glc, glucose; GlcA, glucuronic acid; PGA, potato glycoalkaloids biosynthesis; Rha, rhamnose; S5 α R2, steroid 5 α -reductase 2.

enzymes and enabling efficient substrate channeling (Boccia *et al.*, 2024; Jozwiak *et al.*, 2024). The final products, such as α -solanine and α -tomatine, do not retain the glucuronic acid moiety, suggesting that the glucuronic acid is hydrolyzed at some point in the biosynthetic pathway, although the exact timing of this removal remains unknown. These enzymes, common to both potato and tomato, participate in the biosynthesis of the spirosolane-type aglycone, tomatidenol (Fig. 1). In tomatoes, the C-5,6 double bond from tomatidenol is removed by SI3 β HSD1 and SIS5 α R2, resulting in tomatidine (Akiyama *et al.*, 2019; Lee *et al.*, 2019). Tomatidenol and tomatidine then undergo further modifications catalyzed by four UDP-glycosyltransferases (UGTs) to produce dehydrotomatine and α -tomatine (Itkin *et al.*, 2011, 2013). In potatoes, dioxygenase for solanidane synthesis (DPS) was recently identified as a crucial enzyme for solanidane skeleton formation (Akiyama *et al.*, 2021b). DPS-silenced potato plants show a decrease in α -solanine and α -chaconine levels, accompanied by a significant accumulation of α -solamarine and β -solamarine,

glycosides of tomatidenol. DPS exhibits ring rearrangement activity against α -solamarine/ β -solamarine, forming zwitterchalconine/zwitterchaconine that contain the solanidane scaffold. Following this transformation, the biosynthesis of α -solanine/ α -chaconine is anticipated to be completed through reduction and dehydration from zwitterchalconine/zwitterchaconine.

In this study, we identified two genes, *reductase for potato glycoalkaloid biosynthesis 1* (RPG1) and RPG2, involved in the final steps of α -solanine/ α -chaconine biosynthesis in potato (Fig. 1). RPG1 and RPG2 were co-expressed with previously identified SGA biosynthetic genes in potato. Potato hairy roots with disrupted RPG1 and RPG2 did not produce α -solanine or α -chaconine, but instead accumulated zwitterchalconine and zwitterchaconine. Our *in vitro* assay showed that the sequential reactions catalyzed by RPG1 and RPG2 complete the conversion from zwitterchalconine/zwitterchaconine to α -solanine/ α -chaconine. Here, we have successfully filled the critical missing link in the biosynthetic pathway of a notorious toxin in potato.

Materials and Methods

Chemicals

Authentic samples of α -solanine and α -chaconine were procured from Sigma-Aldrich. α -solamarine and β -solamarine, purified from the diploid potato (*S. tuberosum* L.) clone 97H32-6, had their chemical structures confirmed using nuclear magnetic resonance (NMR) in our laboratory (Shimizu *et al.*, 2020).

Co-expression analysis to survey the candidate genes

We performed a transcriptome analysis using publicly available RNA-seq data from various potato tissues and treatments (PRJEB2430, PRJNA741081, and PRJNA529319). Adapter sequences were trimmed, and low-quality reads were filtered using fastp (Chen *et al.*, 2018). The cleaned fastq files were then mapped to the potato reference genome (DM v.6.1) (Pham *et al.*, 2020). The obtained SAM files were sorted and converted into BAM files using SAMTOOLS (Li *et al.*, 2009). TPM values were quantified for each sample to measure the expression levels using STRINGTIE (Pertea *et al.*, 2016). This dataset was used to perform gene co-expression analysis with the Confeito algorithm (Ogata *et al.*, 2018).

Cloning of Soltu.DM.04G035610 (RPG1) and Soltu.DM.04G035630 (RPG2) cDNAs

Total RNA was extracted using the RNeasy Plant Mini Kit (Qiagen) and the RNase-Free DNase Set (Qiagen) from tuber sprouts of potato (*S. tuberosum* L. cv Sassy). The extracted total RNA was used to synthesize first-strand cDNAs using the ReverTra Ace[®] qPCR RT Master Mix with gDNA remover. The cDNA fragments containing the open reading frames of RPG1 and RPG2 were amplified by reverse transcription polymerase chain reaction, using the first-strand cDNAs as a template, with primers 1 and 2 for RPG1 and primers 3 and 4 for RPG2 (Supporting Information Table S1). The PCR products were cloned into the pCR[®]4 Blunt-TOPO[®] vector (Thermo Fisher Scientific, Waltham, MA, USA).

Expression of the recombinant proteins in *Escherichia coli*

The coding sequences of RPG1 and RPG2 were digested from the pCR[®]4 Blunt-TOPO[®] vector (Thermo Fisher Scientific) using NdeI and SalI. These DNA fragments were then inserted into the NdeI-SalI sites of pCold ProS2 (Takara Bio Inc., Kusatsu, Shiga, Japan). *E. coli* strain BL21 (DE3) (Clontech, Terra Bella Avenue Mountain View, CA, USA), transformed with the constructed plasmid, was cultured at 37°C in LB medium containing ampicillin (50 μ g ml⁻¹) until the OD₆₀₀ reached 0.5. The production of recombinant protein was induced by adding 0.1 mM isopropyl β -D-1-thiogalactopyranoside, and the culture was incubated for 24 h at 15°C. The culture was subsequently centrifuged at 7720 g for 5 min at 4°C, and the cell pellets were resuspended in 4 ml of cold sonication buffer

containing 50 mM Bis-Tris-HCl (pH 7.2), 150 mM NaCl, 10% (v/v) glycerol, and 5 mM dithiothreitol. This solution was sonicated three times for 30 s each on ice using a Bandelin Sonopuls HD 2070 ultrasonic homogenizer type MS73 (Sigma-Aldrich), at a sound intensity of 200 W cm⁻², and then centrifuged at 20 630 g for 10 min at 4°C. The recombinant His-tagged protein in the soluble fraction was purified using a His SpinTrap TALON column (GE Healthcare, Chicago, IL, USA), following the manufacturer's instructions. After two column washes, the adsorbed proteins were eluted twice in 200 μ l of an elution buffer containing 50 mM sodium phosphate (pH 7.4), 30 mM NaCl, and 150 mM imidazole, and the elutions were combined. The purified recombinant proteins were used for subsequent analyses.

Enzymatic synthesis of zwitterosolanine and zwitterchaconine

Zwitterosolanine and zwitterchaconine were produced via DPS enzymatic reaction, utilizing α -solamarine and β -solamarine as substrates, as described previously (Akiyama *et al.*, 2021b). The DPS protein, recombinant His-tagged protein of DPS, was generated using an *E. coli* expression system and purified via Ni-affinity chromatography. The *in vitro* enzyme assay involved a 100 μ l reaction mixture containing 100 mM Bis-Tris-HCl (pH 7.2), 5 mM 2-oxoglutarate, 10 mM sodium ascorbate, 0.2 mM FeSO₄, 25 μ M substrate, and 1 μ g of the purified recombinant DPS. The reaction was initiated by enzyme addition and conducted at 30°C for 1 h, then halted by a 2-min incubation at 90°C.

In vitro activity assay of the recombinant RPG1 and RPG2

Independent assays for zwitterosolanine, zwitterchaconine, 16-iminiumsolanine, 16-iminiumchaconine, 22-iminiumsolanine, or 22-iminiumchaconine with RPG1 or RPG2 utilized a 100 μ l reaction mixture composed of 100 mM Tris-HCl buffer (pH 7.2), 2.5 mM NADPH as coenzymes, 25 μ M of substrate, and 1 μ g of each purified recombinant protein. Simultaneous assays of RPG1 and RPG2 for zwitterosolanine or zwitterchaconine were performed with the same mixture, adding 1 μ g of recombinant RPG1 and RPG2 enzymes, respectively. Reverse reaction assays of RPG1 or RPG2 for α -solanine or α -chaconine were conducted using 100 mM Tris-HCl buffer (pH 8.5), 2.5 mM NAD⁺ as coenzymes, 25 μ M of α -solanine or α -chaconine as substrates, and 1 μ g of each purified recombinant protein. The reaction was initiated by enzyme addition and conducted at 30°C for 1 h, then halted by a 2-min incubation at 90°C. For the assay in Fig. 3(c) (see later), the enzyme assay was conducted with 0.1 μ g of enzyme, and the reactions were stopped at 5, 15, 30 min, and 2 h, respectively.

A 20 μ l sample of the solution was diluted with 180 μ l of MeOH and filtered through a 0.22- μ m polytetrafluoroethylene membrane filter. A 2 μ l aliquot was then analyzed by liquid chromatography-mass spectrometry (LC-MS). The analysis was conducted using an ACQUITY UPLC H-Class System (Waters,

Milford, MA, USA) equipped with an TQ Detector (Waters); data acquisition and analyses were executed using the MASSLYNX 4.1 software (Waters). Each sample was introduced into an ACQUITY UPLC HSS T3 chromatographic column (100 × 2.1 mm, 1 µm; Waters), maintaining a column temperature of 40°C and a flow rate of 0.2 ml min⁻¹. The mass spectra were acquired in positive electrospray ionization mode, with a capillary voltage of 3 kV and a sample cone voltage of 60 V. A mass spectrometry scan mode with a mass range of *m/z* 350–1250 was employed. The mobile phases consisted of water with 0.1% (v/v) formic acid (A), acetonitrile (B), and methanol (C), with a linear gradient elution as follows: transition from solvent A 90% solvent B 5% solvent C 5% to solvent A 40%/solvent B 30%/solvent C 30% over 15 min; shift from solvent A 40%/solvent B 30%/solvent C 30% to solvent A 0%/solvent B 50%/solvent C 50% over 3 min; maintained at solvent A 0%/solvent B 50%/solvent C 50% for 3 min; solvent B and solvent C were then immediately returned to 5%; this was followed by a 5-min re-equilibration period.

Structural determination of the enzymatic reaction products

To ascertain the structure of each enzymatic reaction product catalyzed by the recombinant RPG1 and RPG2, reverse enzymatic reactions were conducted with α-solanine as a substrate using a 400 ml reaction mixture, as previously described with a slight modification; the reactions were performed overnight using each of the purified enzymes in the presence of 2.5 mM NAD⁺. The reaction mixture was incubated at 98°C for 5 min, followed by centrifugation at 9650 g for 10 min. The supernatant was collected, subjected to three extractions with water-saturated butanol, and the resultant butanol layer was corrected and subsequently dried *in vacuo*.

The residue was dissolved in 10% (v/v) aqueous methanol and loaded onto Sep-Pak C18 cartridges (Vac 6 cm³, 1 g; Waters, MA, USA) for purification. For the reverse reaction product of RPG2, stepwise elution was executed using H₂O/MeOH (40% : 60%, 0% : 100%, 5-ml at each step). For the RPG1 reverse reaction product, stepwise elution was performed using H₂O/MeOH (50%:50%, 0%:100%, 5-ml at each step). Each of the 100% methanol fractions was dried and further purified independently using preparative-scale HPLC (Shimadzu, Kyoto, Japan) with the following system: an ODS column (5C18-PAQ, 20 × 250 mm; Nacalai Tesque, Kyoto, Japan) safeguarded by a guard column (5C18-PAQ, 10 × 10 mm; Nacalai Tesque). For the purification of the RPG2 reverse reaction product, isocratic elution was conducted with water/acetonitrile (72 : 28, v/v) containing 0.05% TFA. By contrast, for the purification of the RPG1 reverse reaction product, isocratic elution was performed with water/acetonitrile (75 : 25, v/v) containing 0.05% TFA. The eluents were monitored at 203 nm, and the fractions containing the target compounds were dried *in vacuo*. Subsequently, the fractions containing the target product were concentrated in vacuum, and the resulting dried residue was dissolved in methanol-d₄ (CD₃OD; Sigma-Aldrich). NMR spectra were

recorded using a Bruker AVANCEIII 600 spectrometer (Bruker BioSpin Corp., Billerica, MA, USA) at 800 MHz for ¹H and 201 MHz for ¹³C. The NMR chemical shifts were referenced to tetramethylsilane.

Generation of RPG1- and RPG2-disrupted transgenic potato hairy roots

The knockout potato hairy root for *RPG1* and *RPG2* was generated by targeted genome editing using the CRISPR/Cas9 system. We utilized the CRISPR/Cas9 binary vector pMgP237-2A-GFP to express multiplex gRNAs (Hashimoto *et al.*, 2018; Nakayasu *et al.*, 2018). To design a gRNA target with minimal off-target effect in *RPG1* and *RPG2*, we conducted *in silico* analyses using the web tool design sgRNAs for CRISPRko (<https://portals.broadinstitute.org/gpp/public/analysis-tools/sgna-design>) and CAS-OT software (Xiao *et al.*, 2014). Due to the high sequence similarity between *RPG1* and *RPG2*, it was not feasible to design specific guide RNAs targeting each individually. Consequently, a vector was constructed to simultaneously knock out both *RPG1* and *RPG2*. We selected target sequences named T1 and T2 in the coding region of *RPG1* and *RPG2*. DNA fragments, composed of the gRNA scaffold and tRNA scaffold between two target sequences, were generated by PCR using pMD-gRNA containing gRNA and tRNA scaffolds as a template and primer sets (5 and 6) containing restriction enzyme BsaI sites (Table S1). The gRNAs–tRNAs unit was then inserted into the BsaI site of pMgP237-2A-GFP using Golden Gate Cloning methods to construct the CRISPR/Cas9 vectors, labeled pMgP237-RPGsKO.

The vector pMgP237-RPGsKO was introduced into *Agrobacterium rhizogenes* ATC15834 via electroporation. Transgenic potato hairy roots were generated as previously outlined (Nakayasu *et al.*, 2018). Genomic DNAs were extracted from each hairy root line, and the target region was amplified by PCR using primer sets 7 and 8 listed in Table S1. The PCR-amplified DNA was purified using the Wizard SV Gel and PCR Clean-Up System (Promega). NGS analysis was completed by the Bioengineering Lab (Kanagawa, Japan). Briefly, PCR amplicons were purified using AMPure XP (Beckman Coulter, CA, USA). For the preparation of the pooled sequencing libraries, a second PCR was conducted using the indexing primers. After purification, the libraries were sequenced using the MiSeq system and MiSeq Reagent Kit v3 (Illumina, CA, USA). The obtained data were analyzed using CRISPRESSO2 (Clement *et al.*, 2019).

Analysis of accumulated compound in transgenic potato hairy root

SGAs were extracted from 100 mg of fresh weight harvested from transgenic lines, and the homogenate was subsequently extracted with 300 µl MeOH. Following centrifugation, the supernatant was collected. This extraction process was repeated three times, and the extract was dried *in vacuo*. The residues were then dissolved in 300 µl of MeOH. A 30 µl sample solution was diluted with 270 µl of MeOH and filtered through a 0.22-µm polytetrafluoroethylene membrane filter. A 2 µl aliquot was then

analyzed by UPLC–MS as previously described, with minor modifications. The mobile phases consisted of water with 0.1% (v/v) formic acid (A) and acetonitrile (B). The gradient conditions were as follows: Solvent B ramped linearly from 10% to 25% over 5 min; solvent B increased linearly to 40% over 35 min, then solvent B increased linearly to 100% over 5 min, held at solvent B 100% for 5 min; solvent B then returned immediately to 10%, followed by a 5-min re-equilibration period. The mobile phases consisted of water with 0.1% (v/v) formic acid (A) and acetonitrile (B), using the following gradient conditions: Solvent B increased linearly from 10% to 25% over 5 min, then increased to 40% over 35 min. Subsequently, solvent B was ramped up to 100% over 5 min and held at 100% for an additional 5 min. Solvent B was then immediately returned to 10%, followed by a 5-min re-equilibration period.

Results

Selection of candidate genes for completing solanidane SGAs biosynthesis in potato

We hypothesized that the reduction in the iminium double bond at C-22 is necessary to convert zwitter-solanine/zwitterchaconine to α -solanine/ α -chaconine (Fig. 1). The biosynthetic genes of SGA are under the comprehensive control of the transcription factor GAME9/Jre4, resulting in their coordinated expression (Cárdenas *et al.*, 2016; Thagun *et al.*, 2016). To identify the enzymes that reduce the iminium double bond at C-22, thereby completing the formation of solanidane glycoalkaloids (i.e. α -solanine and α -chaconine) in potato, we performed a gene co-expression analysis with the Confeito algorithm (Ogata *et al.*, 2018) using publicly available next-generation sequencing data from various potato tissues. As a result, we identified a co-expressed gene module composed of 47 genes, which includes most previously identified SGA biosynthetic genes and upstream cholesterol biosynthetic genes (Fig. 2; Table S2). This concise module includes two *NmrA* (nitrogen metabolic regulation A)-like genes, *Soltu.DM.04G035610* and *Soltu.DM.04G035630*. Therefore, we selected *Soltu.DM.04G035610* and *Soltu.DM.04G035630* as candidates and named these genes *RPG1* and *RPG2*, respectively. We successfully amplified the full-length open reading frame sequences of *RPG1* and *RPG2* using cDNAs derived from tuber sprouts of potato (*Solanum tuberosum* cv Sassy). The deduced proteins of *RPG1* share 87.6% amino acid sequence identity with that of *RPG2* (Fig. S1).

Characterization of *RPG1*- and *RPG2*-disrupted potato hairy roots

To verify the role of *RPG1* and *RPG2* in SGA biosynthesis in potato, we endeavored to generate gene-disrupted potato hairy roots using the CRISPR/Cas9 system. Initially, we aimed to create hairy roots with individual knockouts of *RPG1* and *RPG2*. However, the high similarity in the coding regions of *RPG1* and *RPG2* limited the selection of specific guide RNA design regions. Consequently, we selected guide RNAs specific to each gene

within the available regions and incorporated these into CRISPR/Cas9 binary vectors to generate gene-disrupted potato hairy roots. Despite our efforts, we were unable to generate hairy roots in which *RPG1* and *RPG2* were individually knocked out. Therefore, we proceeded to generate potato hairy roots with simultaneous knockout of both *RPG1* and *RPG2* (Fig. 3a). As a result, we obtained two independent lines (#19 and #25) in which both *RPG1* and *RPG2* were disrupted (Fig. 3b). LC-MS analysis of endogenous SGAs revealed that the *RPG1/RPG2* double knockout hairy root (*rpg1_rpg2*) lines showed no accumulation of α -solanine and α -chaconine, the main SGAs in the vector control (VC) potato hairy roots (Fig. 3c). Additionally, *rpg1_rpg2* lines accumulated zwitter-solanine (retention time at 8.6 min) and zwitterchaconine (retention time at 8.8 min), which were undetectable in VC (Fig. 3c). We also observed additional products (marked as * and ** in Fig. 3c) in *rpg1_rpg2* lines, showing parental ion masses at m/z 880 $[M+H]^+$ and 864 $[M+H]^+$ (Fig. S2), respectively. However, due to the very low amounts of these peaks, we were unable to further characterize them structurally.

In vitro functional analysis of the recombinant proteins of *RPG1* and *RPG2*

Each of the recombinant His-tagged proteins of *RPG1* and *RPG2* was prepared using a bacterial expression system in *E. coli* and purified via cobalt-affinity chromatography. The purified *RPG1* and *RPG2* were independently incubated with zwitter-solanine, which was enzymatically synthesized with DPS and α -solamarine (Fig. S3a), as a substrate in the presence of NADPH. The reaction products were then analyzed using LC-MS. In the assay with *RPG1*, two products were observed (Fig. 4a). The major compound (compound A) had a retention time of 13.5 min and exhibited a parental ion mass at m/z 866 $[M+H]^+$, which is 16 mass units smaller than that of the substrate zwitter-solanine: m/z 882 $[M+H]^+$ (Fig. 4). The minor product was identical to the authentic α -solanine in terms of both the retention time and the mass fragmentation pattern (Fig. 4). By contrast, *RPG2* converted zwitter-solanine to a single compound (compound B) with a retention time of 11.3 min and a parental ion mass at m/z 866 $[M+H]^+$ (Fig. 4). Subsequently, we conducted a simultaneous enzyme assay of *RPG1* and *RPG2*, using zwitter-solanine as a substrate and NADPH as a cofactor, under the same enzyme concentration conditions as in the individual enzyme assay experiment shown above. As a result, we observed the complete consumption of zwitter-solanine and the formation of α -solanine as a single product (Fig. 4a). The assays with enzymatically synthesized zwitterchaconine (Fig. S3b) as a substrate yielded essentially the same results as the assays with zwitter-solanine, both in the individual assays and in the simultaneous assay of *RPG1* and *RPG2* (Fig. S4).

Structural determination of compound A and compound B

Next, we sought to determine the chemical structures of compounds A and B. To acquire a large quantity of these

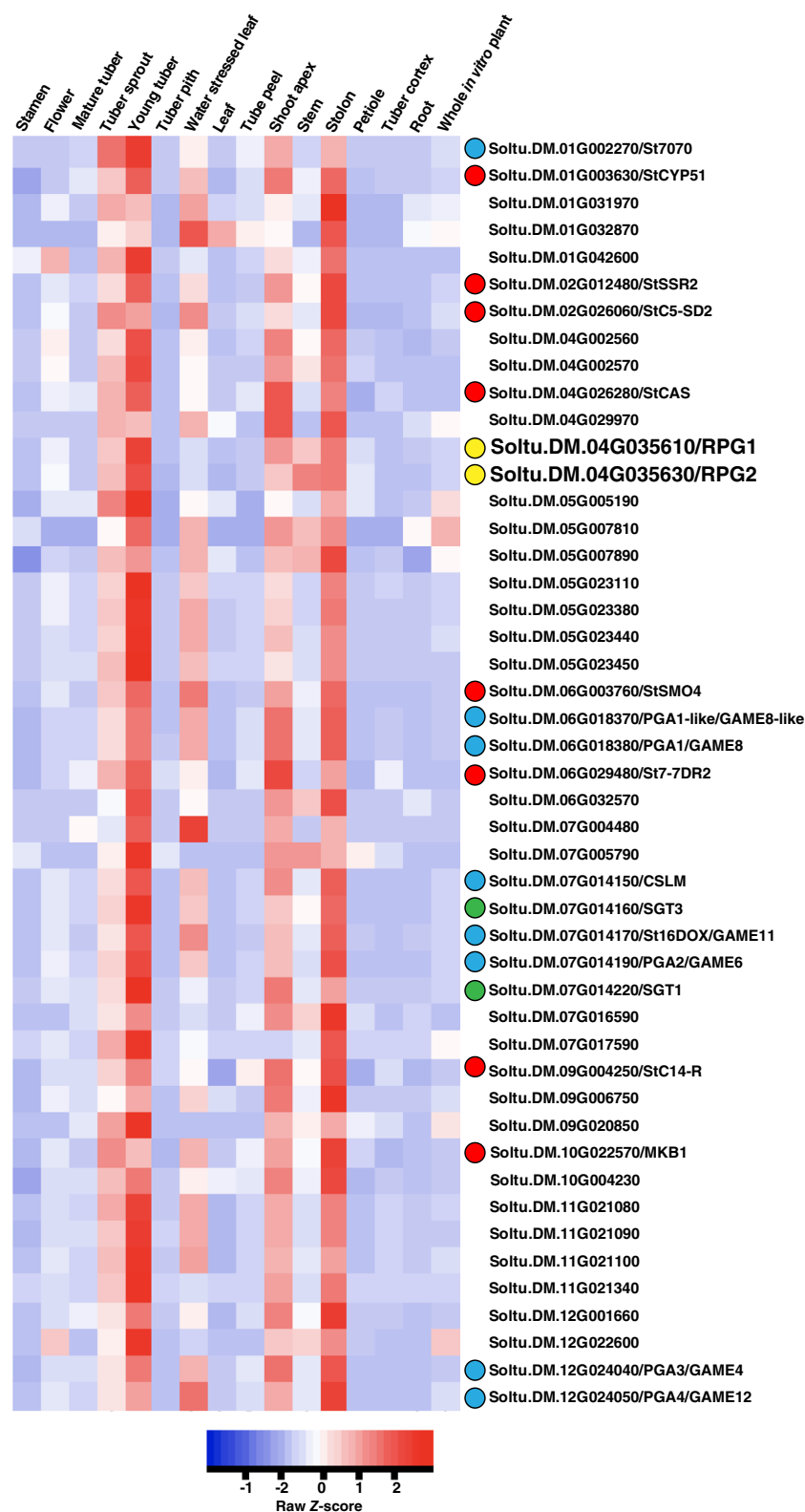


Fig. 2 Gene co-expression analyses of steroidal glycoalkaloid (SGA) biosynthetic genes in potato. All heatmaps represent hierarchical clustering of expression profiles, and expression levels are normalized across conditions. Genes with red dots next to them are SGA biosynthesis genes that function upstream of cholesterol. Blue and green dots indicate the genes involved in aglycon formation steps that function downstream from cholesterol and glycosylation steps, respectively. Green dots represent the gene characterized in this study.

compounds, a significant amount of zwitterosolanine, which serves as the substrate for RPG1 and RPG2, is needed. Zwitterosolanine can be prepared by reacting α -solamarine with DPS. However, α -solamarine, extracted and purified from wild potato leaves in

our laboratory, is available in limited quantities. Consequently, we decided to enzymatically synthesize compounds A and B in large quantities via the reverse reaction of RPG2 and RPG1, using commercially available α -solanine as a substrate (Fig. 5a).

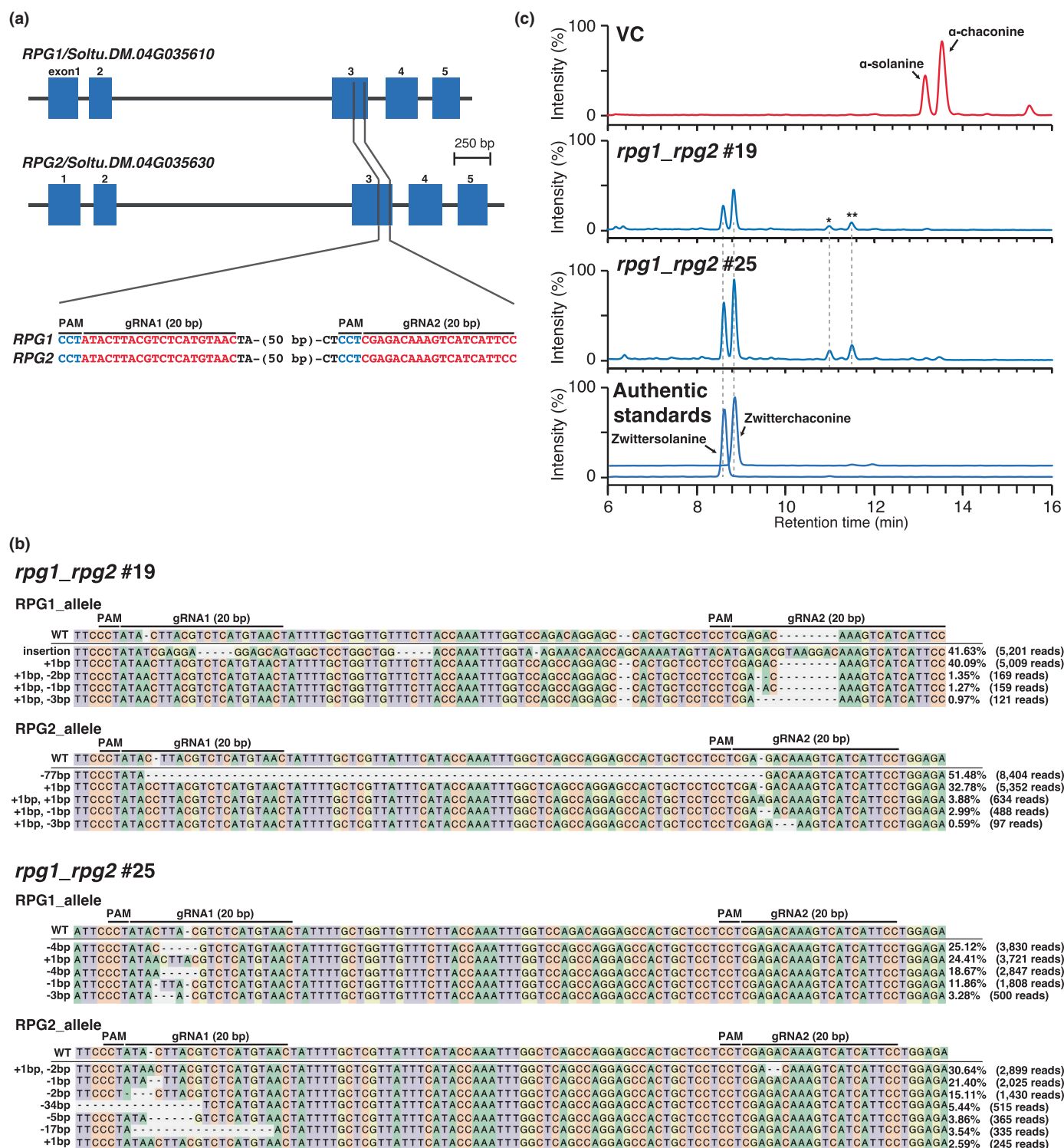


Fig. 3 Characterization of reductase for potato glycoalkaloid biosynthesis 1 (*RPG1*)/*RPG2* double knockout hairy root (*rpg1_rpg2*). (a) The structure of *RPG1* and *RPG2*. The CRISPR/Cas9 target sites are displayed in red letters, followed by the blue protospacer adjacent motif. (b) Genotyping DNA sequences surrounding the *rpg1_rpg2* by next-generation sequencing. The intact wild-type sequences are shown at the top. The number of deleted (–) and inserted (+) nucleotides is indicated on the left. Read counts and allele frequency are displayed on the right. (c) Steroidal glycoalkaloid profiles determined by liquid chromatography-mass spectrometry (LC-MS) in the *rpg1_rpg2*. The total ion current chromatogram obtained in positive ionization mode with a full-scan range of 350–1250 *m/z* is shown. Refer to Supporting Information Fig. S2 for mass spectra of these new compounds (* and **).

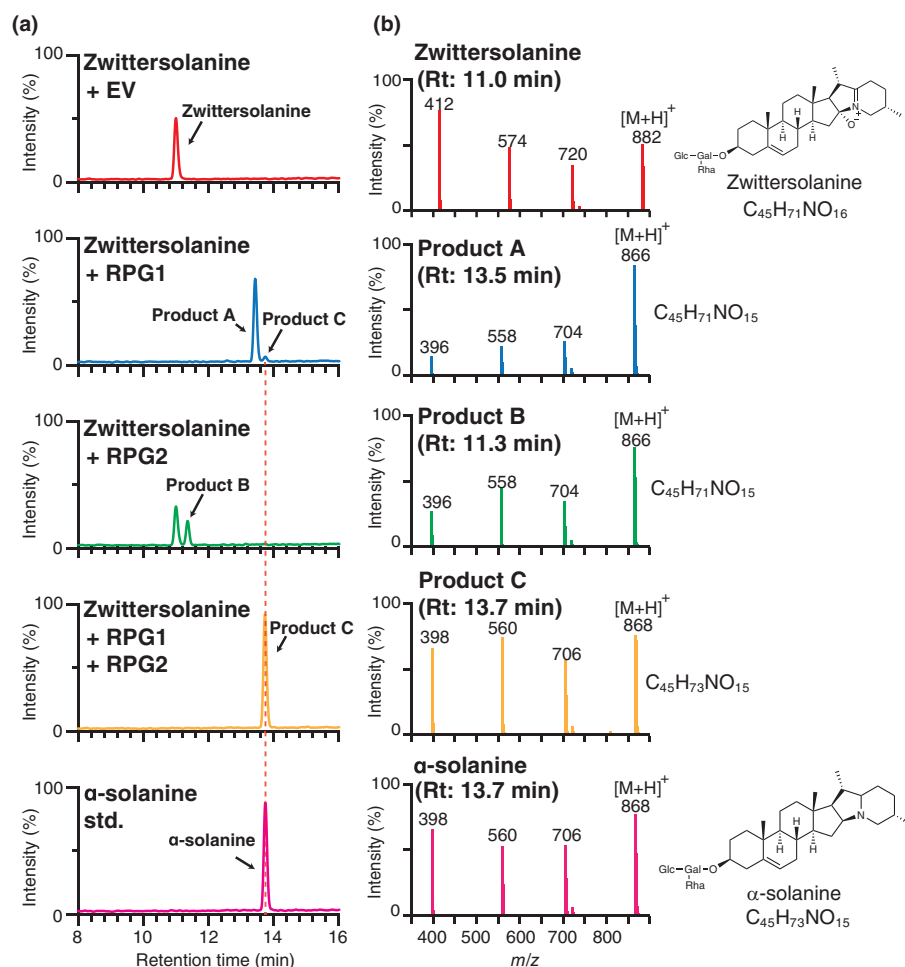


Fig. 4 The enzymatic activity of reductase for potato glycoalkaloid biosynthesis 1 (RPG1) and RPG2. (a) Liquid chromatography-mass spectrometry (LC-MS) analysis of the reaction products from the recombinant RPG1 and RPG2 proteins with zwitterosolanine as a substrate. The total ion current chromatogram, obtained in positive ionization mode with a full-scan range of 350–1250 *m/z*, is shown. EV indicates a negative control reaction performed using a purified protein fraction from *Escherichia coli* cells transformed with an empty pCold ProS2 vector. (b) Mass spectrum of the peaks at a retention time of 11.0 min (substrate, zwitterosolanine), 13.5 min (product A), 11.3 min (product B), 13.7 min (product C), and 13.7 min (authentic standard of α-solanine). The structures and chemical formulas of zwitterosolanine and α-solanine are presented alongside their corresponding mass spectra. For products A, B, and C, the predicted chemical formulas are shown adjacent to their respective mass spectra.

Incubation of α-solanine with RPG2 in the presence of NAD⁺ resulted in the formation of a new peak, identical to the product of RPG1 reacted with zwitterosolanine (compound A) in terms of retention time and mass pattern (Fig. 5b,c). Similarly, the reverse reaction product with RPG1 and α-solanine was confirmed to be identical to compound B (Fig. 5b,c). We prepared respective enzymatic reaction products on a milligram-scale reaction. Each obtained reaction product was purified using open-column chromatography and reverse-phase HPLC and then analyzed using NMR spectroscopy (Figs S5–S18). The structures of the reaction products were determined as shown in Fig. 5d (Table S3). Compound A forms an iminium ion with the nitrogen and the C-16 carbon atoms, while compound B forms an iminium ion with the nitrogen and the C-22 carbon atoms. We named the respective compounds 16-iminiumsolanine and 22-iminiumsolanine (Fig. 5d).

Reaction order of RPG1 and RPG2 in the pathway to α-solanine

While RPG1 alone can convert zwitterosolanine to α-solanine, a more efficient conversion was observed when RPG1 and RPG2 were assayed simultaneously (Fig. 4a). This led us to hypothesize that the conversion of zwitterosolanine to α-solanine is more

efficient through consecutive reactions involving RPG1 and RPG2. To test this hypothesis, we conducted *in vitro* assays using 16-iminiumsolanine and 22-iminiumsolanine as substrates. A reaction involving RPG2, NADPH, and 16-iminiumsolanine as a substrate resulted in the production of α-solanine. Similarly, incubation of RPG1 with 22-iminiumsolanine in the presence of NADPH led to the formation of α-solanine (Fig. 6a). Moreover, 16-iminiumchaconine, obtained by reacting zwitterchaconine with RPG1, was further metabolized by RPG2, resulting in the formation of α-chaconine. Additionally, 22-iminiumchaconine, obtained by reacting zwitterchaconine with RPG2, was further metabolized by RPG1, leading to the formation of α-chaconine (Fig. S19). These *in vitro* assay results suggest that α-solanine/α-chaconine could be biosynthesized from zwitterosolanine/zwitterchaconine via two pathways, with 16-iminiumsolanine and 22-iminiumsolanine serving as intermediates.

Next, to determine which of the two pathways is dominant, we performed assays of RPG1 and RPG2 using zwitterosolanine as a substrate, reducing the enzyme concentration 10-fold compared with the assay performed in Fig. 6(a). The results showed that in the case of RPG1, 16-iminiumsolanine formation was observed after a 5-min reaction, and after 2 h, the substrate was completely consumed. Conversely, with RPG2, only a small amount of 22-iminiumsolanine was observed after a 30-min reaction, and even

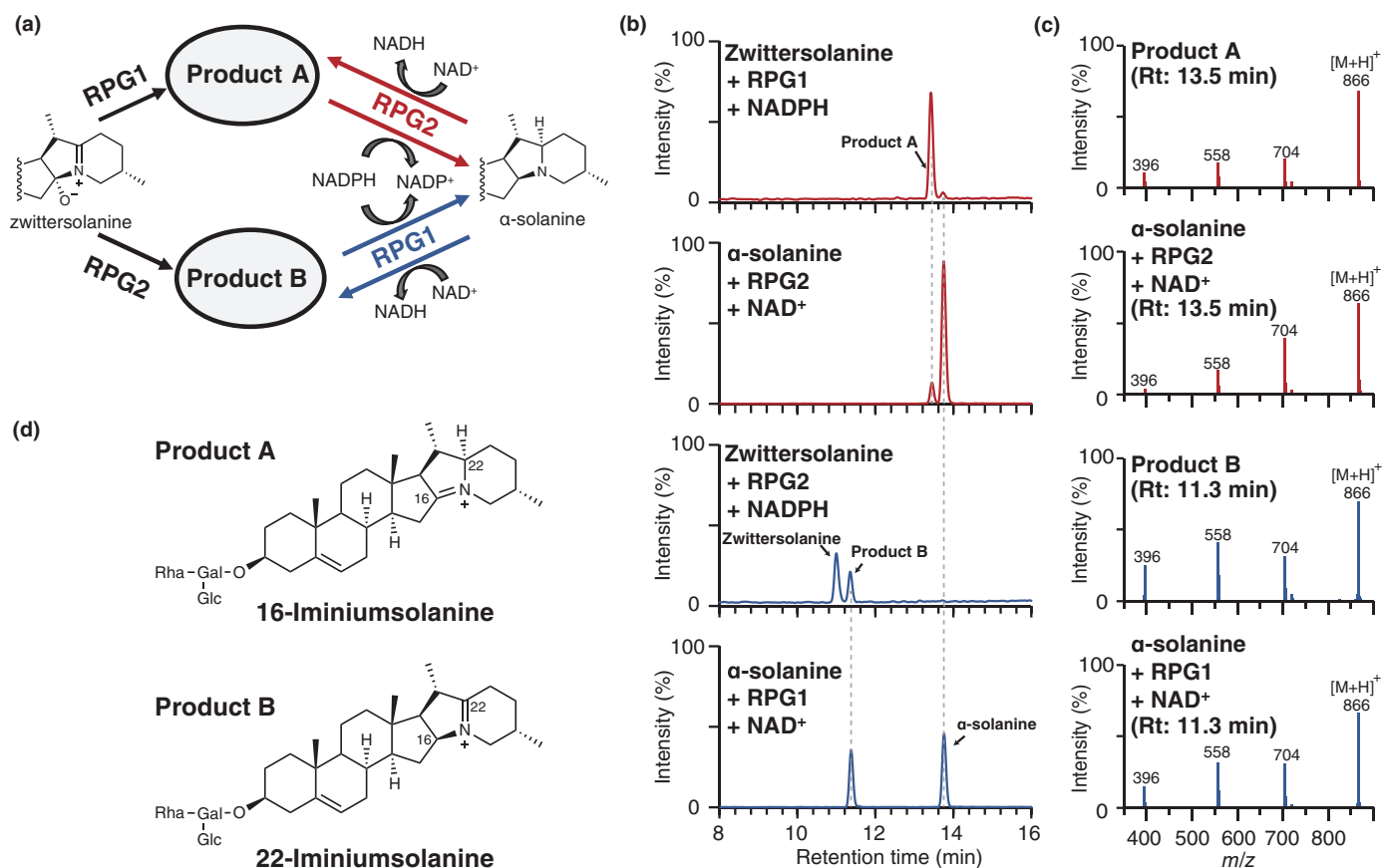


Fig. 5 Preparation of product A and product B by reverse reaction of reductase for potato glycoalkaloid biosynthesis 1 (RPG1) and RPG2 and structural determination of the reaction products. (a) Schematic of enzymatic preparation of product A and product B by the reverse reaction of RPGs. (b) Liquid chromatography-mass spectrometry (LC-MS) analysis of the reaction products from the recombinant RPG1 and RPG2 proteins with α -solanine as a substrate in the presence of NAD^+ . The total ion current chromatogram obtained in positive ionization mode with a full-scan range of 350–1250 m/z is shown. (c) Mass spectrum of the peaks at a retention time of 13.5 min (product A produced by the reaction of RPG1 with zwitterosolanine), 13.5 min (obtained by incubation of α -solanine with RPG2 and NAD^+), 11.3 min (product B produced by RPG2 with zwitterosolanine), and 11.3 min (obtained by incubation of α -solanine with RPG1 and NAD^+). (d). Chemical structures of product A and product B determined by nuclear magnetic resonance.

after 2 h, a significant portion of the substrate remained unconsumed (Fig. 6b). These results suggest that the conversion of zwitterosolanine to 16-iminiumsolanine by RPG1 is a faster reaction than the conversion of zwitterosolanine to 22-iminiumsolanine by RPG2 (Fig. 6c).

Discussion

In this study, we report the identification of RPG1 and RPG2, which are responsible for the final reaction steps of α -solanine/ α -chaconine biosynthesis in potato. Our *in vitro* assay and NMR characterization of the reaction products revealed that RPG1 catalyzes the conversion of zwitterosolanine/zwitterchaconine to 16-iminiumsolanine/16-iminiumchaconine, while RPG2 catalyzes the conversion of zwitterosolanine/zwitterchaconine to 22-iminiumsolanine/22-iminiumchaconine (Figs 4, S4–S18; Tables S3, S4). Furthermore, we demonstrated that 16-iminiumsolanine/16-iminiumchaconine were further converted to α -solanine/ α -chaconine by RPG2, and 22-iminiumsolanine/22-iminiumchaconine were further converted to α -solanine/ α -

chaconine by RPG1 (Figs 6a, S19). Additional evidence of their function *in planta* was obtained through gene knockout of both RPG1 and RPG2, resulting in a complete abolishment of α -solanine and α -chaconine production and accumulation of zwitterosolanine and zwitterchaconine in potato hairy roots (Fig. 3). As described previously, our *in vitro* assay showed that the conversion of zwitterosolanine/zwitterchaconine to α -solanine/ α -chaconine could occur through dual pathways. However, the reaction of RPG2 converting zwitterosolanine to 22-iminiumsolanine is much slower than the reaction converting zwitterosolanine to 16-iminiumsolanine catalyzed by RPG1 (Fig. 6b). Therefore, it is expected that the pathway in which RPG1 functions first, that is via 16-iminiumsolanine, predominates during SGA biosynthesis in potato plants. Indeed, the isolation of 16-iminiumsolanine and 16-iminiumchaconine from potato tuber has been reported (Baur *et al.*, 2022). These observations support that 16-iminiumsolanine and 16-iminiumchaconine are intermediates of the SGA biosynthetic pathway in potato.

Both RPG1 and RPG2 encode proteins similar to NmrA. NmrA-like proteins are a group of negative transcriptional

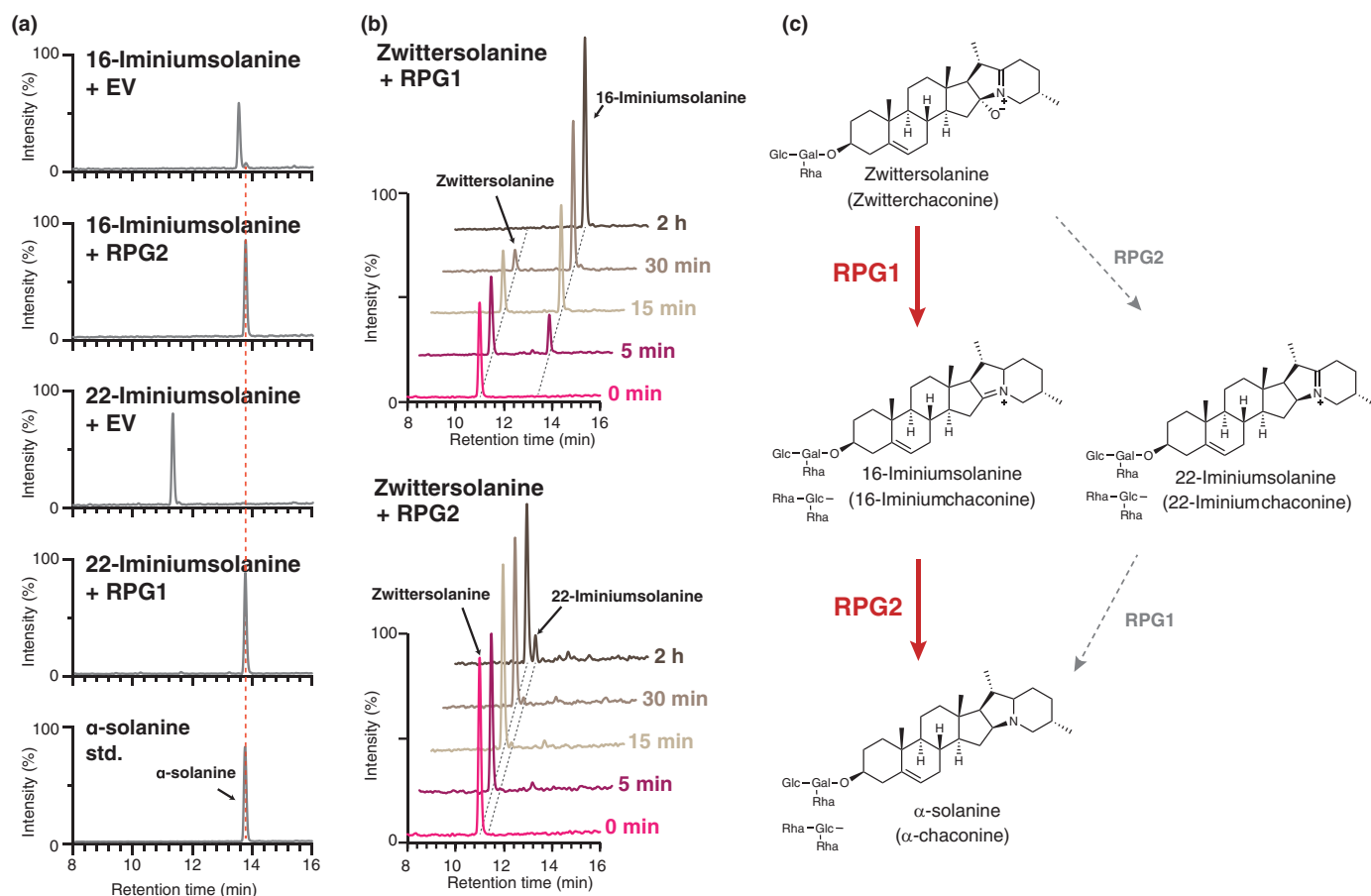


Fig. 6 The enzymatic activity of reductase for potato glycoalkaloid biosynthesis 1 (RPG1) and RPG2. (a) Liquid chromatography-mass spectrometry (LC-MS) analysis of the reaction products from the recombinant RPG1 and RPG2 proteins with 16-iminiumsolanine and 22-iminiumchaconine as substrates. The total ion current chromatogram obtained in positive ionization mode with a full-scan range of 350–1250 m/z is shown. (b) The reaction time course of RPG1 and RPG2 using zwitterсоланин as a substrate was also studied. (c) The biosynthetic pathways for α-solanine/α-chaconine from zwitterсоланин/zwitterchaconine in potato (*Solanum tuberosum*) predicted based on the results of the *in vitro* assay. Red solid arrows indicate the primary reaction pathways, while gray dashed arrows represent minor reaction pathways.

regulators functioning in the nitrogen catabolite pathway. They possess a nicotinamide adenine dinucleotide (phosphate)-binding motif and exhibit unexpected similarity with the structure of short-chain dehydrogenase/reductase family enzymes (Stammers *et al.*, 2001). Some proteins in this family are known to function as bifunctional oxidoreductase/diels-aldolase. In plants, enzymes with NmrA-like domains, such as phenylcoumaran benzylic ether reductase (PCBR), involved in lignan biosynthesis, and isoflavone reductase (IFR), involved in flavonoid biosynthesis, have been reported (Paiva *et al.*, 1991, 1994; Gang *et al.*, 1999; Min *et al.*, 2003). PCBR and IFR catalyze the NADPH-dependent reduction in phenylcoumaran benzylic ether and isoflavone, respectively. RPG1 converts zwitterсоланин/zwitterchaconine to 16-iminiumsolanine/16-iminiumchaconine. This conversion is hypothesized to begin with the reduction in the iminium double bond at C-22, catalyzed by RPG1, to form a hemiaminal intermediate. This is followed by spontaneous dehydration, resulting in the formation of 16-iminium products (Fig. S20).

Recent studies have highlighted that tandem gene duplication plays a significant role in generating the structural diversity of

SGAs (Akiyama *et al.*, 2021a,b, 2022). Our findings reveal that RPG1 and RPG2 are adjacent in the potato genome, with two additional NmrA-like genes located nearby (Fig. S21). By contrast, the corresponding region in the tomato genome contains only one NmrA-like gene (Soly04g080550), the deduced protein of which exhibits 87.4% amino acid similarity to RPG1 and 90.5% similarity to RPG2. Similarly, in eggplant, there is a single NmrA-like gene (SMEL4.1_04g021550) in the region, and the deduced protein of SMEL4.1_04g021550 shows 84.8% amino acid similarity to RPG1, 87.5% similarity to RPG2, and 92.2% similarity to Soly04g080550. Given that the production of solanidane SGAs (i.e. α-solanine and α-chaconine) is confined to potato and wild potato species within the *Solanum* genus, it is hypothesized that the ancestral NmrA-like gene underwent duplication post the speciation of potato, leading to the acquisition of new functions and enabling the biosynthesis of α-solanine and α-chaconine.

In addition to *Solanum* species, certain species of *Veratrum*, a genus of monocotyledonous plants, are also known to produce steroidal alkaloids. Notably, *Veratrum* species synthesize

solanidine, which is the aglycone of α -solanine and α -chaconine (Kaneko *et al.*, 1976, 1977). In *Veratrum* species, the biosynthetic pathway of solanidine is distinct from that in Potato (*S. tuberosum*) (Augustin *et al.*, 2015; Nakayasu *et al.*, 2017). It is hypothesized that in *Veratrum* species, solanidine is biosynthesized via verazine (Kaneko *et al.*, 1976, 1977). Augustin *et al.* identified four genes (*CYP90B27*, *CYP94N1*, *GABAT1*, and *CYP90G1*) from *Veratrum californicum* that catalyze the first six reactions in the conversion of cholesterol to verazine (Augustin *et al.*, 2015). The pathway and genes involved in the conversion of verazine to solanidine have not yet been identified, and it remains unclear whether a reduction reaction, similar to that observed in the pathway of potato, is required. The identification of the solanidine biosynthetic pathway in *Veratrum* species will offer valuable insights into the evolutionary scenario underlying solanidine production in two evolutionarily distinct lineages: potato (*Solanum* spp., eudicots) and *Veratrum* spp. (monocots).

The structures of SGA are highly diverse. For example, unripe tomato fruits contain a high concentration of toxic α -tomatine, which contributes to their bitterness. During fruit ripening, α -tomatine undergoes a series of four enzymatic reactions, ultimately being metabolized into the tasteless and nontoxic esculeoside A (Nakayasu *et al.*, 2020; Szymański *et al.*, 2020; Akiyama *et al.*, 2021a; Sonawane *et al.*, 2023). Additionally, certain accessions of the wild potato species *Solanum chacoense* produce leptines, rare glycoalkaloids with a solanidane skeleton (Sinden *et al.*, 1986). Leptines have been reported to contribute to resistance against the Colorado potato beetle, a major pest of potato and other *Solanum* crops comprising pepper, tomato, and eggplant (Sinden *et al.*, 1986). Thus, structural diversity of SGAs underpins their wide range of biological activities. The production of solanidane-type SGAs by potatoes may have conferred evolutionary advantages as part of their survival strategy. Interestingly, while the reaction catalyzed by DPS alone can produce zwitter-solanine/zwitter-chaconine with a solanidane skeleton, these compounds are further metabolized by RPG1 and RPG2 into α -solanine/ α -chaconine. The biological significance of this additional metabolic step is intriguing. Although the toxicity of zwitter-solanine/zwitter-chaconine against herbivorous insects or other external threats remains unclear, further studies, for example, using RPG1- and RPG2-deficient mutants, may provide insights into the evolutionary rationale behind potato plants' production of α -solanine/ α -chaconine.

Our findings broaden the understanding of how the structural diversity of SGAs is generated. SGAs exhibit diverse bioactivities depending on their structure. Our research could pave the way for tailoring SGA structures within *Solanum* plants, potentially enabling the development of *Solanum* crop varieties with reduced toxicity or enhanced resistance to diseases and pests.

Acknowledgements

Parts of the experimental measurements were carried out using a Bruker AVANCEIII 800 and 600 NMR spectrometers in the Joint Usage/Research Center (JURC) at the Institute for Chemical Research, Kyoto University. The authors are greatly indebted

to K. Ohmine and A. Maeno (Kyoto University) for performing instrumental analyses. This work was in part supported by Grant-in-Aid for Transformative Research Areas (A) Forecasting Biosynthesis (Grant no. JP23H04555 for MM) and JSPS Grant-in-Aid for Japan Society for the Promotion of Science Research Fellow (19J10750 to RA).








Competing interests

None declared.

Author contributions

RA and MM planned and designed the experiments. RA, DT and AN performed protein expression and enzyme assay. RA, DT and AN performed the purification of the enzymatic reaction products, and BW performed NMR analysis of the enzymatic reaction products. RA, DT and AN performed LC-MS/MS analysis of SGAs. RA and NA performed the generation of the transgenic potato hairy roots. RA and MM wrote the paper with input from all authors. NU, TM, KS and YS supervised research. All authors read and approved the final version of the manuscript.

ORCID

Ryota Akiyama  <https://orcid.org/0000-0003-2116-4226>
Masaharu Mizutani  <https://orcid.org/0000-0002-4321-0644>
Toshiya Muranaka  <https://orcid.org/0000-0003-1058-2473>
Kazuki Saito  <https://orcid.org/0000-0001-6310-5342>
Yukihiro Sugimoto  <https://orcid.org/0000-0002-8767-9671>
Naoyuki Umemoto  <https://orcid.org/0000-0001-5507-0848>
Bunta Watanabe  <https://orcid.org/0000-0003-3645-5712>

Data availability

The data supporting the findings of this study are presented in Figs 1–6, S1–S21; Tables S1–S4 of this article.

References

- Akiyama R, Lee HJ, Nakayasu M, Osakabe K, Osakabe Y, Umemoto N, Saito K, Muranaka T, Sugimoto Y, Mizutani M. 2019. Characterization of steroid 5 α -reductase involved in α -tomatine biosynthesis in tomatoes. *Plant Biotechnology* 36: 253–263.
- Akiyama R, Nakayasu M, Umemoto N, Kato J, Kobayashi M, Lee HJ, Sugimoto Y, Iijima Y, Saito K, Muranaka T *et al.* 2021a. Tomato E8 encodes a C-27 hydroxylase in metabolic detoxification of α -tomatine during fruit ripening. *Plant and Cell Physiology* 62: 775–783.
- Akiyama R, Watanabe B, Kato J, Nakayasu M, Lee HJ, Umemoto N, Muranaka T, Saito K, Sugimoto Y, Mizutani M. 2022. Tandem gene duplication of dioxygenases drives the structural diversity of steroidal glycoalkaloids in the tomato clade. *Plant and Cell Physiology* 63: 981–990.
- Akiyama R, Watanabe B, Nakayasu M, Lee HJ, Kato J, Umemoto N, Muranaka T, Saito K, Sugimoto Y, Mizutani M. 2021b. The biosynthetic pathway of potato solanidanes diverged from that of spiro-solanines due to evolution of a dioxygenase. *Nature Communications* 12: 1300.
- Augustin MM, Ruzicka DR, Shukla AK, Augustin JM, Starks CM, O'Neil-Johnson M, McKain MR, Evans BS, Barrett MD, Smithson A *et al.* 2015.

- Elucidating steroid alkaloid biosynthesis in *Veratrum californicum*: production of verazine in Sf9 cells. *The Plant Journal* 82: 991–1003.
- Baur S, Bellé N, Hausladen H, Wurzer S, Brehm L, Stark TD, Hückelhoven R, Hofmann T, Dawid C. 2022. Quantitation of toxic steroidal glycoalkaloids and newly identified saponins in post-harvest light-stressed potato (*Solanum tuberosum* L.) varieties. *Journal of Agricultural and Food Chemistry* 70: 8300–8308.
- Boccia M, Kessler D, Seibt W, Grabe V, Rodríguez López CE, Grzech D, Heinicke S, O'Connor SE, Sonawane PD. 2024. A scaffold protein manages the biosynthesis of steroidal defense metabolites in plants. *Science* 386: 1366–1372.
- Cárdenas PD, Sonawane PD, Pollier J, Vanden Bossche R, Dewangan V, Weithorn E, Tal L, Meir S, Rogachev I, Malitsky S *et al.* 2016. GAME9 regulates the biosynthesis of steroidal alkaloids and upstream isoprenoids in the plant mevalonate pathway. *Nature Communications* 7: 10654.
- Chen S, Zhou Y, Chen Y, Gu J. 2018. FASTP: an ultra-fast all-in-one FASTQ preprocessor. *Bioinformatics* 34: i884–i890.
- Clement K, Rees H, Canver M, Gehrke JM, Farouni R, Hsu JY, Cole MA, Liu DR, Joung KJ, Bauer DE *et al.* 2019. CRISPResso2 provides accurate and rapid genome editing analysis. *Nature Biotechnology* 37: 220–224.
- Friedman M. 2002. Tomato glycoalkaloids: role in the plant and in the diet. *Journal of Agricultural and Food Chemistry* 50: 5751–5780.
- Friedman M. 2006. Potato glycoalkaloids and metabolites: roles in the plant and in the diet. *Journal of Agricultural and Food Chemistry* 54: 8655–8681.
- Friedman M. 2015. Chemistry and anticarcinogenic mechanisms of glycoalkaloids produced by eggplants, potatoes, and tomatoes. *Journal of Agricultural and Food Chemistry* 63: 3323–3337.
- Friedman M, McDonald GM, Filadelfi-Keszi M. 1997. Potato glycoalkaloids: chemistry, analysis, safety, and plant physiology. *Critical Reviews in Plant Sciences* 16: 55–132.
- Gang DR, Kasahara H, Xia ZQ, Vander Mijnsbrugge K, Bauw G, Boerjan W, Montagu VM, Davin LB, Lewis NG. 1999. Evolution of plant defense mechanisms: relationships of phenylcoumaran benzylic ether reductases to pinoresinol-lariciresinol and isoflavone reductases. *Journal of Biological Chemistry* 274: 7516–7527.
- Hashimoto R, Ueta R, Abe C, Osakabe Y, Osakabe K. 2018. Efficient multiplex genome editing induces precise, and self-ligated type mutations in tomato plants. *Frontiers in Plant Science* 9: 916.
- Itkin M, Heinig U, Tzfadia O, Bhide AJ, Shinde B, Cardenas PD, Bocobza SE, Unger T, Malitsky S, Finkers R *et al.* 2013. Biosynthesis of antinutritional alkaloids in solanaceous crops is mediated by clustered genes. *Science* 341: 175–179.
- Itkin M, Rogachev I, Alkan N, Rosenberg T, Malitsky S, Masini L, Meir S, Iijima Y, Aoki K, de Vos R *et al.* 2011. GLYCOALKALOID METABOLISM1 is required for steroidal alkaloid glycosylation and prevention of phytotoxicity in tomato. *Plant Cell* 23: 4507–4525.
- Jozwiak A, Panda S, Akiyama R, Yoneda A, Umemoto N, Saito K, Yasumoto S, Muranaka T, Ghara SA, Kazachkova Y *et al.* 2024. A cellulose synthase-like protein governs the biosynthesis of Solanum alkaloids. *Science* 386: eadq5721.
- Kaneko K, Tanaka MW, Mitsuhashi H. 1976. Origin of nitrogen in the biosynthesis of solanidine by *Veratrum grandiflorum*. *Phytochemistry* 15: 1391–1393.
- Kaneko K, Tanaka MW, Mitsuhashi H. 1977. Dormantinol, a possible precursor in solanidine biosynthesis, from budding *Veratrum grandiflorum*. *Phytochemistry* 16: 1247–1251.
- Lee HJ, Nakayasu M, Akiyama R, Kobayashi M, Miyachi H, Sugimoto Y, Umemoto N, Saito K, Muranaka T, Mizutani M. 2019. Identification of a 3 β -hydroxysteroid dehydrogenase/3-ketosteroid reductase involved in α -tomatine biosynthesis in tomato. *Plant and Cell Physiology* 60: 1304–1315.
- Li H, Handsaker B, Wysoker A, Fennell T, Ruan J, Homer N, Marth G, Abecasis G, Durbin R, Subgroup 1000 Genome Project Data Processing. 2009. The Sequence Alignment/Map format and SAMTOOLS. *Bioinformatics* 25: 2078–2079.
- Milner SE, Brunton NP, Jones PW, O'Brien NM, Collins SG, Maguire AR. 2011. Bioactivities of glycoalkaloids and their aglycones from Solanum species. *Journal of Agricultural and Food Chemistry* 59: 3454–3484.
- Min T, Kasahara H, Bedgar DL, Youn B, Lawrence PK, Gang DR, Halls SC, Park H, Hilsenbeck JL, Davin LB *et al.* 2003. Crystal structures of pinoresinol-lariciresinol and phenylcoumaran benzylic ether reductases and their relationship to isoflavone reductases. *Journal of Biological Chemistry* 278: 50714–50723.
- Nakayasu M, Akiyama R, Kobayashi M, Lee HJ, Kawasaki T, Watanabe B, Urakawa S, Kato J, Sugimoto Y, Iijima Y *et al.* 2020. Identification of α -tomatine 23-hydroxylase involved in the detoxification of a bitter glycoalkaloid. *Plant and Cell Physiology* 61: 21–28.
- Nakayasu M, Akiyama R, Lee HJ, Osakabe K, Osakabe Y, Watanabe B, Sugimoto Y, Umemoto N, Saito K, Muranaka T *et al.* 2018. Generation of α -solanine-free hairy roots of potato by CRISPR/Cas9 mediated genome editing of the St16DOX gene. *Plant Physiology and Biochemistry* 131: 70–77.
- Nakayasu M, Umemoto N, Akiyama R, Ohya K, Lee HJ, Miyachi H, Watanabe B, Muranaka T, Saito K, Sugimoto Y *et al.* 2021. Characterization of C-26 aminotransferase, indispensable for steroidal glycoalkaloid biosynthesis. *The Plant Journal* 108: 81–92.
- Nakayasu M, Umemoto N, Ohya K, Fujimoto Y, Lee HJ, Watanabe B, Muranaka T, Saito K, Sugimoto Y, Mizutani M. 2017. A dioxygenase catalyzes steroid 16 α -hydroxylation in steroidal glycoalkaloid biosynthesis. *Plant Physiology* 175: 120–133.
- Ogata Y, Mannen K, Kotani Y, Kimura N, Sakurai N, Shibata D, Suzuki H. 2018. CONFETOGUI: a toolkit for size-sensitive community detection from a correlation network. *PLoS ONE* 13: 1–18.
- Paiva NL, Edwards R, Sun Y, Hrazdina G, Dixon RA. 1991. Stress responses in alfalfa (*Medicago sativa* L.). 11. Molecular cloning and expression of alfalfa isoflavone reductase, a key enzyme of isoflavonoid phytoalexin biosynthesis. *Plant Molecular Biology* 17: 653–667.
- Paiva NL, Sun YJ, Dixon RA, Vanetten HD, Hrazdina G. 1994. Molecular cloning of isoflavone reductase from pea (*Pisum sativum* L.): evidence for a 3R-Isoflavanone intermediate in (+)-Pisatin biosynthesis. *Archives of Biochemistry and Biophysics* 312: 501–510.
- Pertea M, Kim D, Pertea GM, Leek JT, Salzberg SL. 2016. Transcript-level expression analysis of RNA-seq experiments with HISAT, StringTie and Ballgown. *Nature Protocols* 11: 1650–1667.
- Pham GM, Hamilton JP, Wood JC, Burke JT, Zhao H, Vaillancourt B, Ou S, Jiang J, Buell CR. 2020. Construction of a chromosome-scale long-read reference genome assembly for potato. *GigaScience* 9: gaa100.
- Sawai S, Ohya K, Yasumoto S, Seki H, Sakuma T, Yamamoto T, Takebayashi Y, Kojima M, Sakakibara H, Aoki T *et al.* 2014. Sterol side chain reductase 2 is a key enzyme in the biosynthesis of cholesterol, the common precursor of toxic steroidal glycoalkaloids in potato. *Plant Cell* 26: 3763–3774.
- Shakya R, Navarre DA. 2008. LC-MS analysis of solanidane glycoalkaloid diversity among tubers of four wild potato species and three cultivars (*Solanum tuberosum*). *Journal of Agricultural and Food Chemistry* 56: 6949–6958.
- Shimizu K, Kushida A, Akiyama R, Lee HJ, Okamura Y, Masuda Y, Sakata I, Tanino K, Matsukida S, Inoue T *et al.* 2020. Hatching stimulation activity of steroidal glycoalkaloids toward the potato cyst nematode, globodera rostochiensis. *Plant Biotechnology* 37: 1–7.
- Sinden SL, Sanford LL, Cantelo WW, Deahl KL. 1986. Leptine glycoalkaloids and resistance to the Colorado potato beetle (Coleoptera: Chrysomelidae) in Solanum chacoense. *Environmental Entomology* 15: 1057–1062.
- Sonawane PD, Gharat SA, Jozwiak A, Barbole R, Heinicke S, Almekias-Siegl E, Meir S, Rogachev I, Connor SEO, Giri AP *et al.* 2023. A BAHD-type acyltransferase concludes the biosynthetic pathway of non-bitter glycoalkaloids in ripe tomato fruit. *Nature Communications* 14: 4540.
- Stammers DK, Ren J, Leslie K, Nichols CE, Lamb HK, Cocklin S, Dodds A, Hawkins AR. 2001. The structure of the negative transcriptional regulator NmrA reveals a structural superfamily which includes the short-chain dehydrogenase/reductases. *EMBO Journal* 20: 6619–6626.
- Szymański J, Bocobza S, Panda S, Sonawane P, Cárdenas PD, Lashbrooke J, Kamble A, Shahaf N, Meir S, Bovy A *et al.* 2020. Analysis of wild tomato introgression lines elucidates the genetic basis of transcriptome and metabolome variation underlying fruit traits and pathogen response. *Nature Genetics* 52: 1111–1121.

Thagun C, Imanishi S, Kudo T, Nakabayashi R, Ohyama K, Mori T, Kawamoto K, Nakamura Y, Katayama M, Nonaka S *et al.* 2016. Jasmonate-responsive ERF transcription factors regulate steroidal glycoalkaloid biosynthesis in tomato. *Plant and Cell Physiology* 57: 961–975.

Umemoto N, Nakayasu M, Ohyama K, Yotsu-Yamashita M, Mizutani M, Seki H, Saito K, Muranaka T. 2016. Two cytochrome P450 monooxygenases catalyze early hydroxylation steps in the potato steroid glycoalkaloid biosynthetic pathway. *Plant Physiology* 171: 2458–2467.

Xiao A, Cheng Z, Kong L, Zhu Z, Lin S, Gao G, Zhang B. 2014. CasOT: a genome-wide Cas9/gRNA off-target searching tool. *Bioinformatics* 30: 1180–1182.

Supporting Information

Additional Supporting Information may be found online in the Supporting Information section at the end of the article.

Fig. S1 Alignment of the amino acid sequences of reductase for potato glycoalkaloid biosynthesis 1 (RPG1) and RPG2.

Fig. S2. Mass spectrum of product* and product** in Fig. 5.

Fig. S3 Liquid chromatography-mass spectrometry analysis of the reaction products from the recombinant dioxygenase for solanidane synthesis (DPS) and St7070 proteins with α -solanarine and β -solanarine as substrates, respectively.

Fig. S4 Reductase for potato glycoalkaloid biosynthesis 1 (RPG1) and RPG2 enzymatic activity using zwitterchaconine as a substrate.

Fig. S5 ^1H nuclear magnetic resonance spectra of 16-iminiumsolanine.

Fig. S6 ^{13}C nuclear magnetic resonance of 16-iminiumsolanine.

Fig. S7 Correlation spectroscopy analysis of 16-iminiumsolanine.

Fig. S8 Rotating frame nuclear Overhauser effect spectroscopy analysis of 16-iminiumsolanine.

Fig. S9 Heteronuclear single quantum coherence analysis of 16-iminiumsolanine.

Fig. S10 Heteronuclear multiple bond coherence analysis of 16-iminiumsolanine.

Fig. S11 Observed heteronuclear multiple bond coherence, correlation spectroscopy, and rotating frame nuclear Overhauser effect spectroscopy for 16-iminiumsolanine.

Fig. S12 ^1H nuclear magnetic resonance spectra of 22-iminiumsolanine.

Fig. S13 ^{13}C nuclear magnetic resonance spectra of 22-iminiumsolanine.

Fig. S14 Correlation spectroscopy analysis of 22-iminiumsolanine.

Fig. S15 Rotating frame nuclear Overhauser effect spectroscopy analysis of 22-iminiumsolanine.

Fig. S16 Heteronuclear single quantum coherence analysis of 22-iminiumsolanine.

Fig. S17 Heteronuclear multiple bond coherence analysis of 22-iminiumsolanine.

Fig. S18 Observed heteronuclear multiple bond coherence, correlation spectroscopy, and rotating frame nuclear Overhauser effect spectroscopy for 22-iminiumsolanine.

Fig. S19 Reductase for potato glycoalkaloid biosynthesis 1 (RPG1) and RPG2 enzymatic activity using 16-iminiumchaconine and 22-iminiumchacanonine as substrates.

Fig. S20 Putative reaction mechanism of reductase for potato glycoalkaloid biosynthesis 1 (RPG1) and RPG2.

Fig. S21 Genomic organization of the RPG homologous genes in potato, tomato, and eggplant.

Table S1 Primers used in this paper.

Table S2 List of genes included in the co-expression module.

Table S3 ^{13}C and ^1H assignment of the reductase for potato glycoalkaloid biosynthesis 1 (RPG1) and RPG2 enzymatic reaction product in CD_3OD (TMS; 800 MHz for ^1H ; 201 MHz for ^{13}C).

Table S4 ^{13}C and ^1H assignment of the solatriose moiety of the reductase for potato glycoalkaloid biosynthesis 1 (RPG1) and RPG2 enzymatic reaction products in CD_3OD (TMS; 800 MHz for ^1H ; 201 MHz for ^{13}C).

Please note: Wiley is not responsible for the content or functionality of any Supporting Information supplied by the authors. Any queries (other than missing material) should be directed to the *New Phytologist* Central Office.

Disclaimer: The New Phytologist Foundation remains neutral with regard to jurisdictional claims in maps and in any institutional affiliations.